ALEPH 94-056
PHYSIC 94-050
G. Bujosa & J. Carr
20.04.1994

Measuring p_t in Semileptonic B Decays with Vertices

Guillaume Bujosa and John Carr, CPP Marseille

1 Introduction

We describe a method to measure lepton transverse momentum in B hadron semileptonic decays by taking the B flight direction as the line joining the primary vertex and the B decay vertex. With cuts to ensure a reasonable resolution in p_t, the method is shown to give a typical resolution of 0.15 Gev/c in p_t for an efficiency of about 45% for events which have vertices formed from tracks with VDET hits.

We examine the method using Monte-Carlo events for $B \to \rho^0 l\nu$ and $B \to D^{*+} l\nu$ decays and compare this measurement of p_t with the standard measures using the jet for the B flight direction. For the plots showing reconstructed variables in this note the primary vertex is taken from the QFNDIP package in ALPHA and all tracks in the secondary vertex are required to have at least one VDET hit in each view $r\phi$ and z. We will show that compared to the jet p_t methods, which are used largely for selecting pure b hadron samples, this vertex method has dramatically better resolution for actually measuring the lepton transverse momentum.

The method has been developed with the intention of using it to measure V_{ub} in semileptonic B decays. The difference in the kinematic endpoint of the centre-of-mass lepton momenta (2.3 Gev/c for $B \to cl\nu$ and 2.6 GeV/c for $B \to ul\nu$) is retained in the p_t of the lepton in the lab, so if the endpoint of p_t can be accurately measured, V_{ub} and V_{cb} events can be separated given sufficient statistics.

2 Method

Once a secondary vertex is found for a particular event, the method is simply to take the B direction as the line between the primary and secondary vertices and to calculate the lepton p_t from the angle between this direction and the lepton momentum. With the definitions as in figure 1(a):

$$p_t = p \sin \epsilon,$$

and for each event its error is calculated from:

$$(\frac{\sigma_{p_t}}{p_t})^2 = (\frac{\sigma_p}{p})^2 + (\frac{\sigma_\epsilon}{\tan\epsilon})^2.$$

The contribution to σ_{p_t} from σ_p is small compared to that from σ_ϵ. At present σ_ϵ is calculated geometrically as indicated in figure 1(b), using:

$$\sigma_\epsilon = \frac{\sqrt{u^T(M_{PV} + M_{SV})u}}{d}$$

where u is a unit vector in the plane of the B direction and the lepton momentum which is normal to the B direction, M_{PV} and M_{SV} are the covariance matrices of the primary and secondary vertices and d is the distance between the primary and secondary vertices.

If the secondary vertex reconstructed is a good approximation to the B decay point, then this method gives p_t with an accurate error on an event by event basis. Figure 2 shows p_t pull distributions (reconstructed minus truth divided by the above error) for Monte Carlo events of type $B \to \rho^0 l\nu$ with no cuts and with cuts on decay length and on σ_{p_t}. The B decay vertex is formed between the lepton and the $\pi^+\pi^-$ from the ρ^0 decay. The distributions are well fitted by Gaussians of nearly unit widths (1.02 - 1.18) showing that the calculated error on p_t is a reasonable approximation for all events. This calculated error could be used as a cut or as a weight in an analysis to reduce the influence of poorly measured events.

Figures 3 and 4 show the distributions of σ_{p_t} for Monte Carlo $B \to \rho^0 l\nu$ and $B \to D^{*+} l\nu$ events respectively. The $D^{*+} l\nu$ events are reconstructed in the decay mode $D^{*+} \to D^0\pi_s, D^0 \to K\pi$ with the B vertex formed between the lepton and the neutral D^0 track ignoring the π_s. The arrows indicate the position of the $\sigma_{p_t} < 0.3$ Gev/c used for all later plots. After this cut the mean error in p_t is 0.11 Gev/c for $\rho^0 l\nu$ and 0.12 Gev/c for $D^{*+} l\nu$. Together with the decay length cut, this requirement gives an efficiency of 45% for events within the VDET acceptance (after correcting for the low B lifetime in the Monte Carlo used).

3 Comparison with standard p_t measures

In figures 5 and 6 we compare the resolution of the vertex method with that obtained from the p_t measure taking the B direction as that of the jet both with and without the lepton included in the jet. For these plots the resolution is taken as p_t reconstructed minus the Monte Carlo truth calculated from the true B direction and the true lepton direction. The cuts have been applied for the distributions for jet methods even though these methods do not need them. The distribution for the vertex method is centered at zero while those from the two jet definitions are shifted from zero in different senses. Table 1 shows the root mean square of the various distributions in figures 5 and 6; clearly there is

	$\rho l\nu$ RMS Δp_t GeV/c	$D^* l\nu$ RMS Δp_t GeV/c
p_t Vertex	0.18	0.20
p_t Jet (lepton excl.)	1.1	0.67
p_t Jet (lepton incl.)	0.52	0.42

Table 1: RMS of the distibutions for p_t(reconstructed)- p_t(true) in figs 5 and 6.

a large improvement in precision in p_t with the vertex method particularly for the $\rho l\nu$ mode where the jet direction is badly defined.

As a final comparison figures 7 and 8 compare reconstructed and true p_t distributions with the three measurement methods for the two channels. It is seen that with the vertex method the high p_t end points of the spectra are distinct and it could be possible to distinguish events of the type $B \to \rho l\nu$ at high p_t using this method. Clearly with the standard definition of p_t this would be difficult.

4 Conclusion

We have shown the vertex p_t method gives a measurement of p_t with a typical precision of 0.15 GeV/c after cuts which have an efficiency of about 45% for events for which good vertices have been found using tracks with the VDET. With this method the error is calculated for each event and could be used in the analysis. Finally, we believe there is some hope of measuring V_{ub} in semileptonic decays using the kinematic p_t limit and work is in progress on the data to see if indeed the method is feasible.

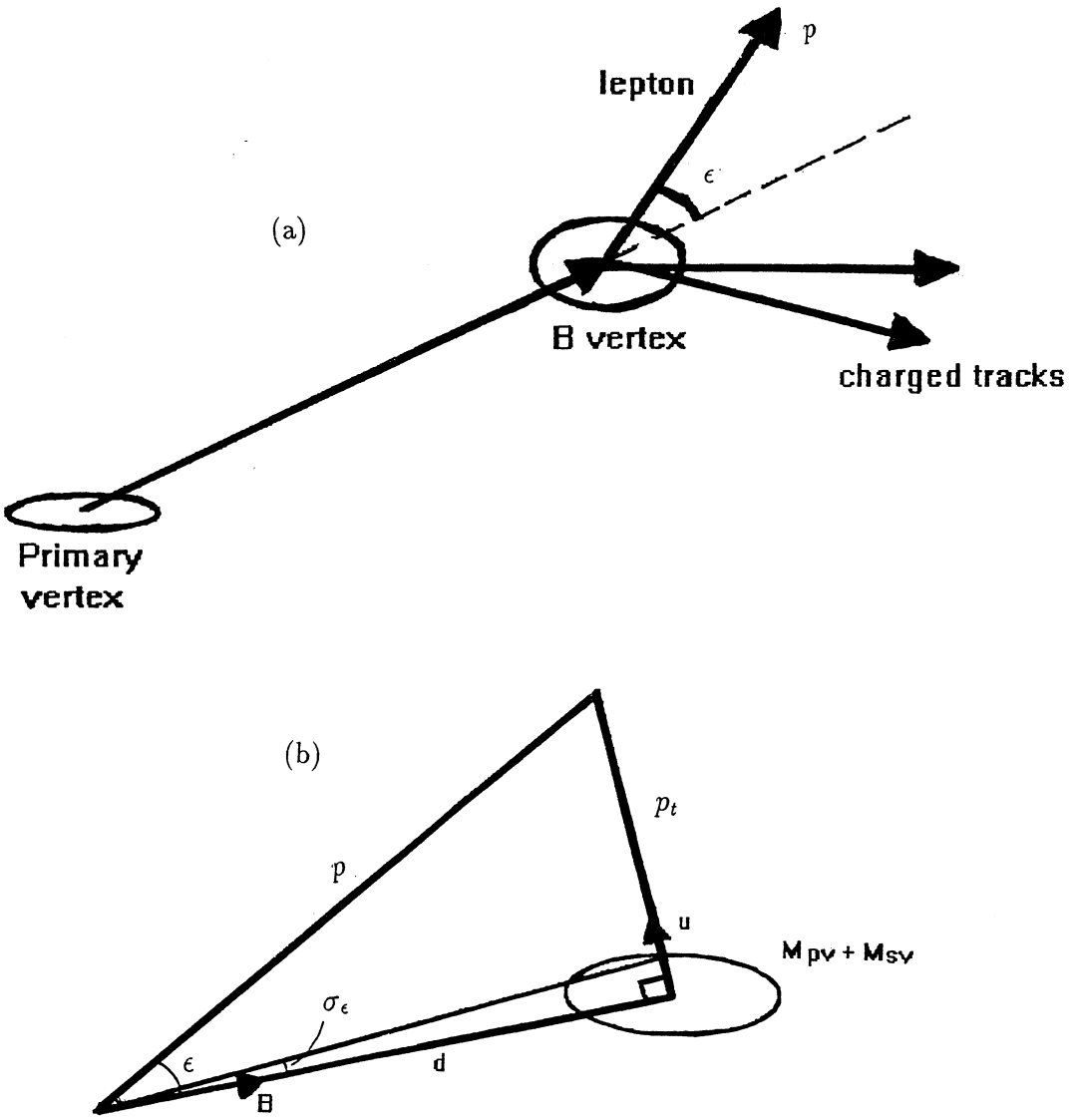

Figure 1: (a) Schematic of method, (b) Definition of variables

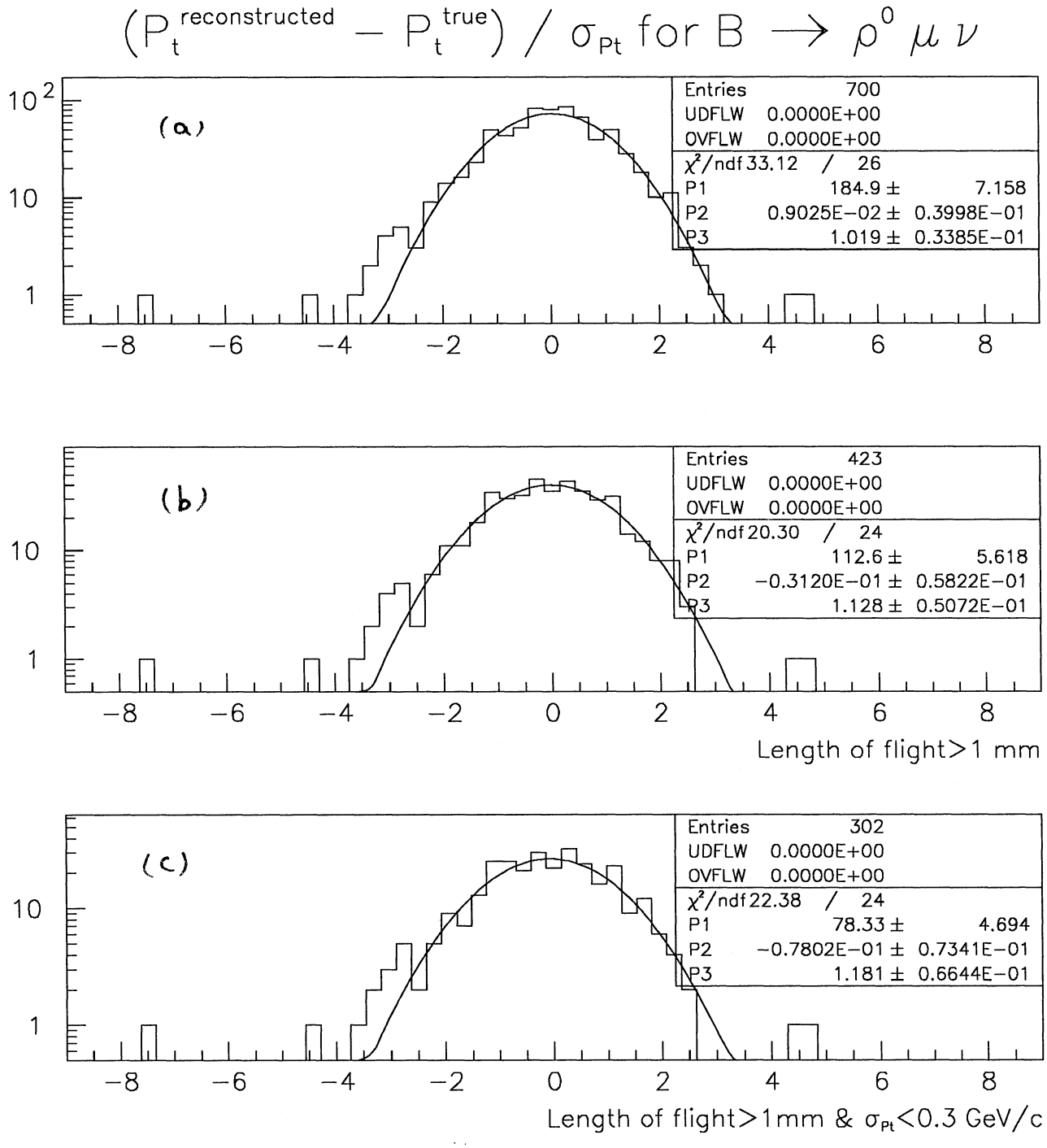

Figure 2: Pull distribution for p_t from Monte Carlo truth for $B \rightarrow \rho^0 l\nu$ events. (a) All events, (b) with cut on decay length to be greater than $1mm$, (c) plus cut on calculated $\sigma_{p_t} < 0.3$ GeV/c.

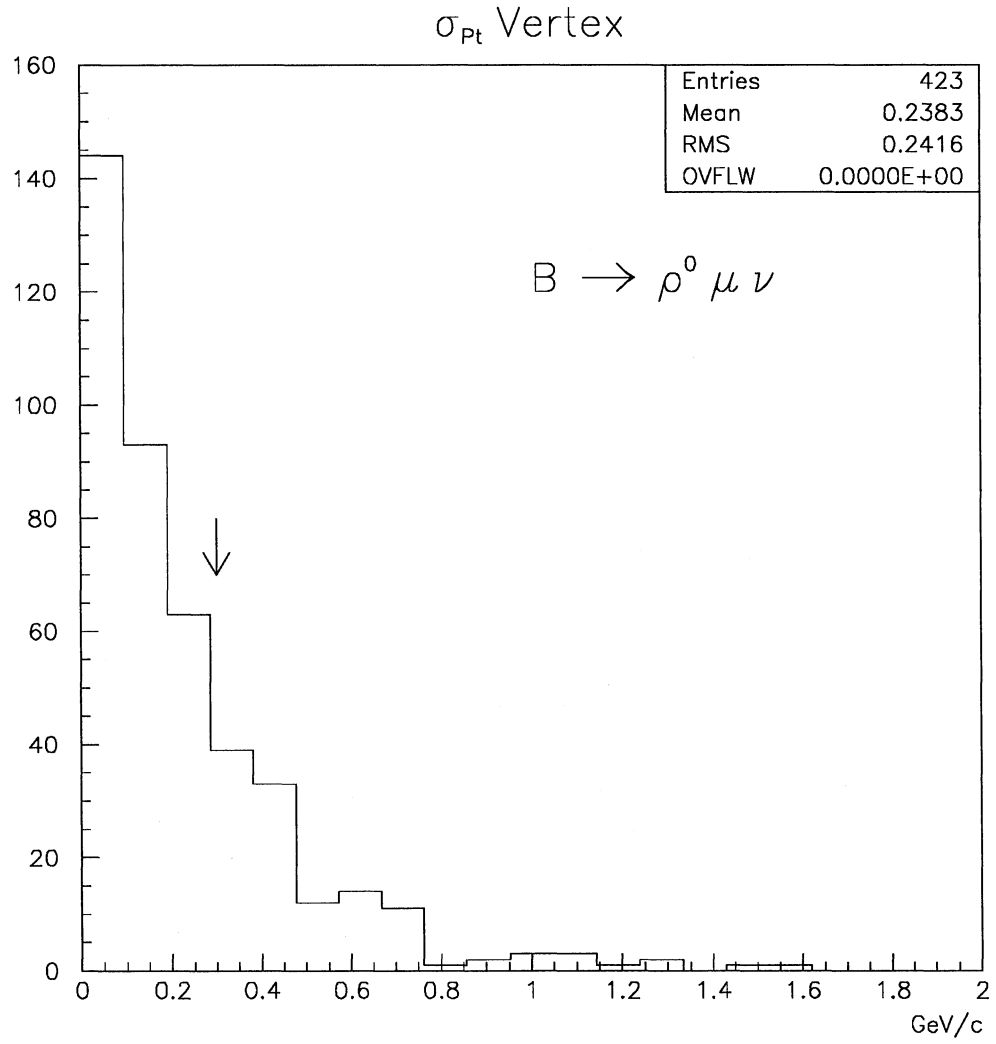

Figure 3: Distribution of calculated error in p_t for $B \rightarrow \rho^0 l\nu$ events, after a decay length cut of $1mm$. The arrow indicates the position of the cut applied for later plots.

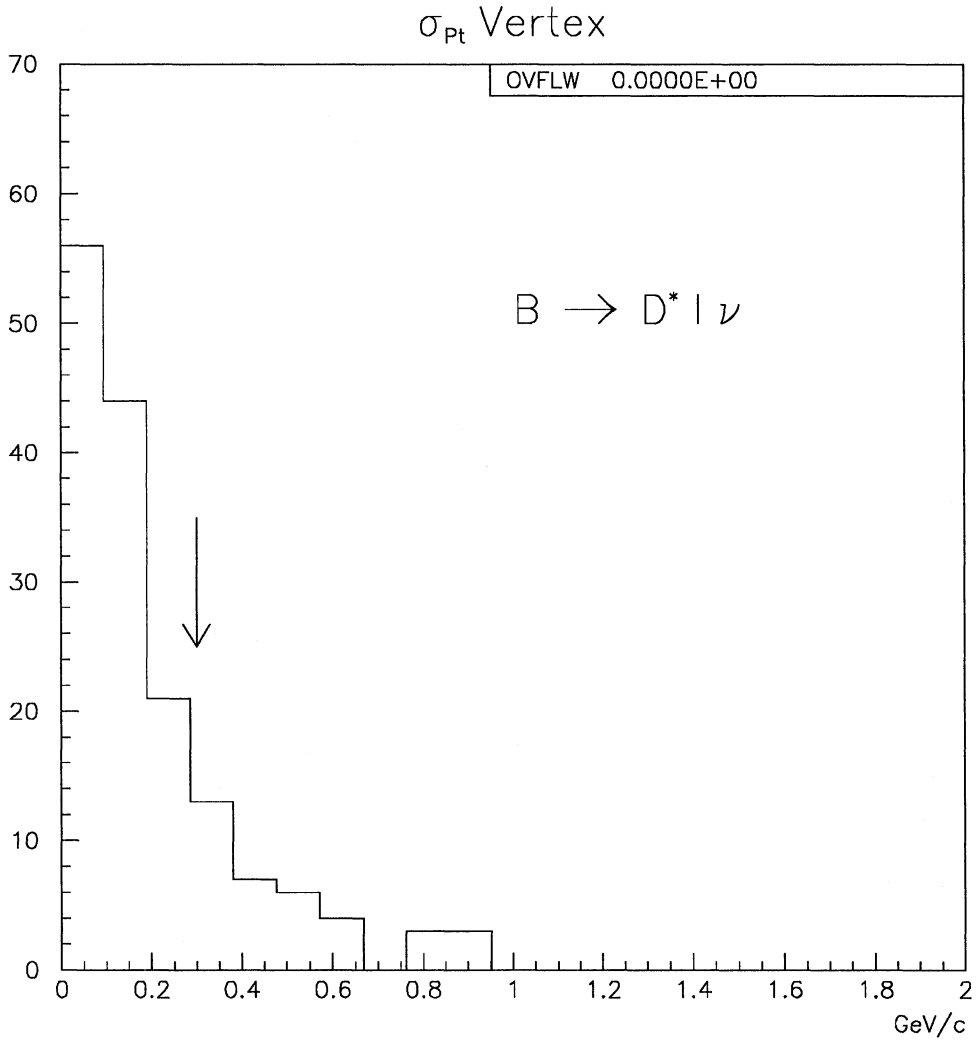

Figure 4: Distribution of calculated error in p_t for $B \rightarrow D^{*+} l\nu$ events, after a decay length cut of $1mm$.

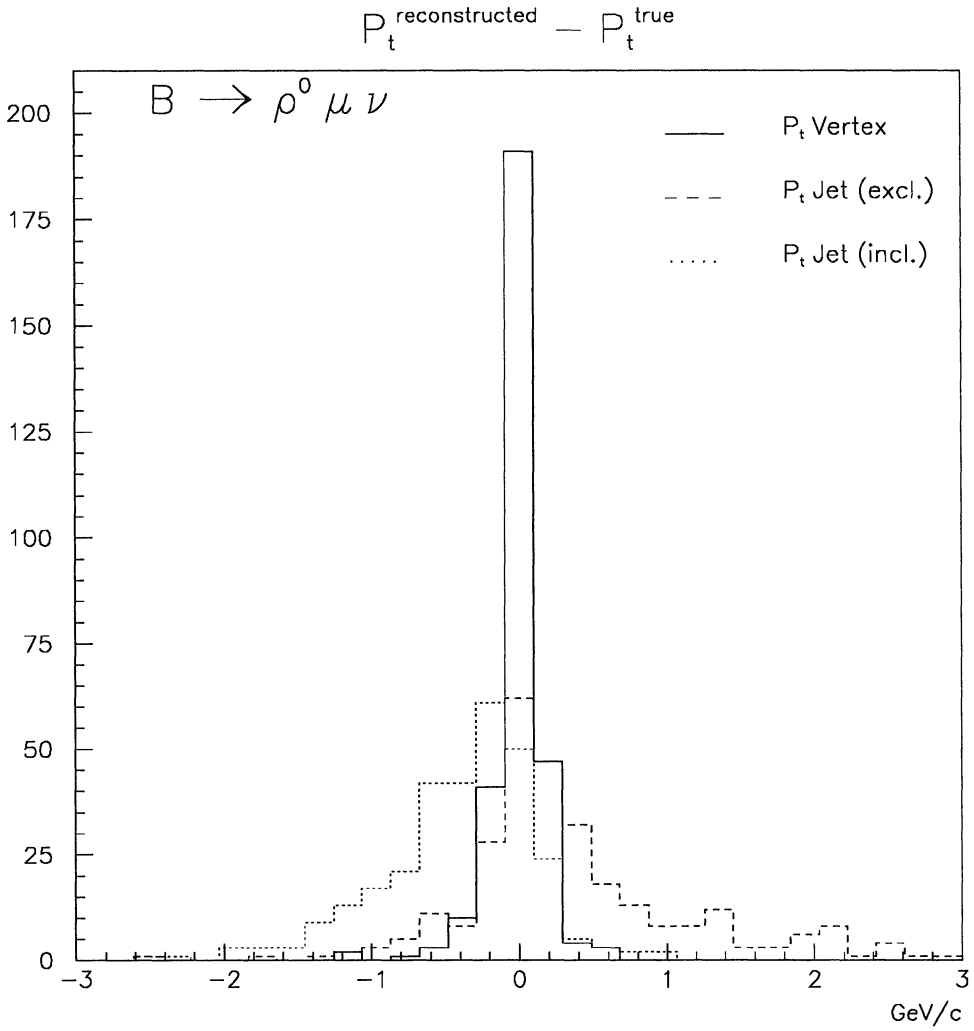

Figure 5: Distribution of p_t (reconstructed) - p_t (true) for $B \rightarrow \rho^0 l\nu$ events, with the vertex p_t method and the standard jet p_t methods. For these and all later distributions events are required to have a decay length of $> 1mm$ and a calculated $\sigma_{p_t} < 0.3$ Gev/c.

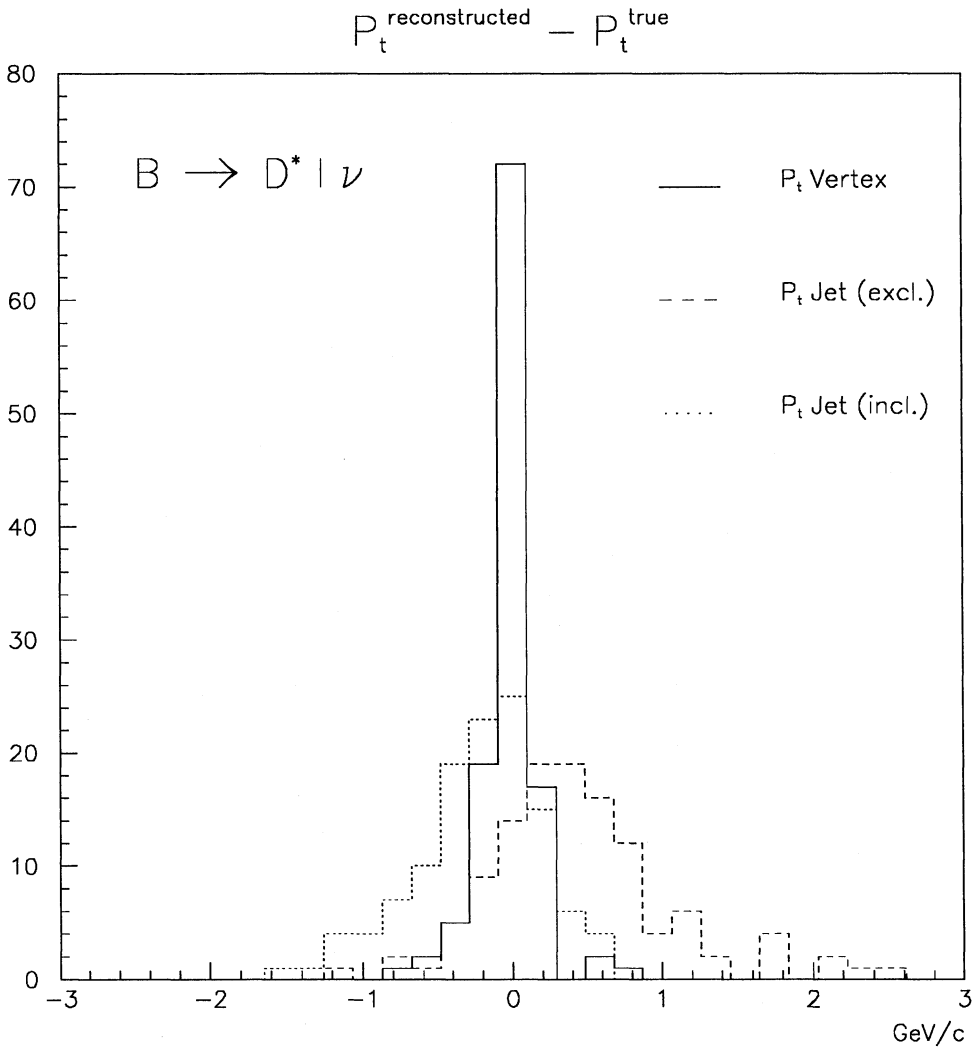

Figure 6: Distribution of p_t (reconstructed) - p_t (true) for $B \to D^{*+} l\nu$ events, with the vertex p_t method and the standard jet p_t methods.

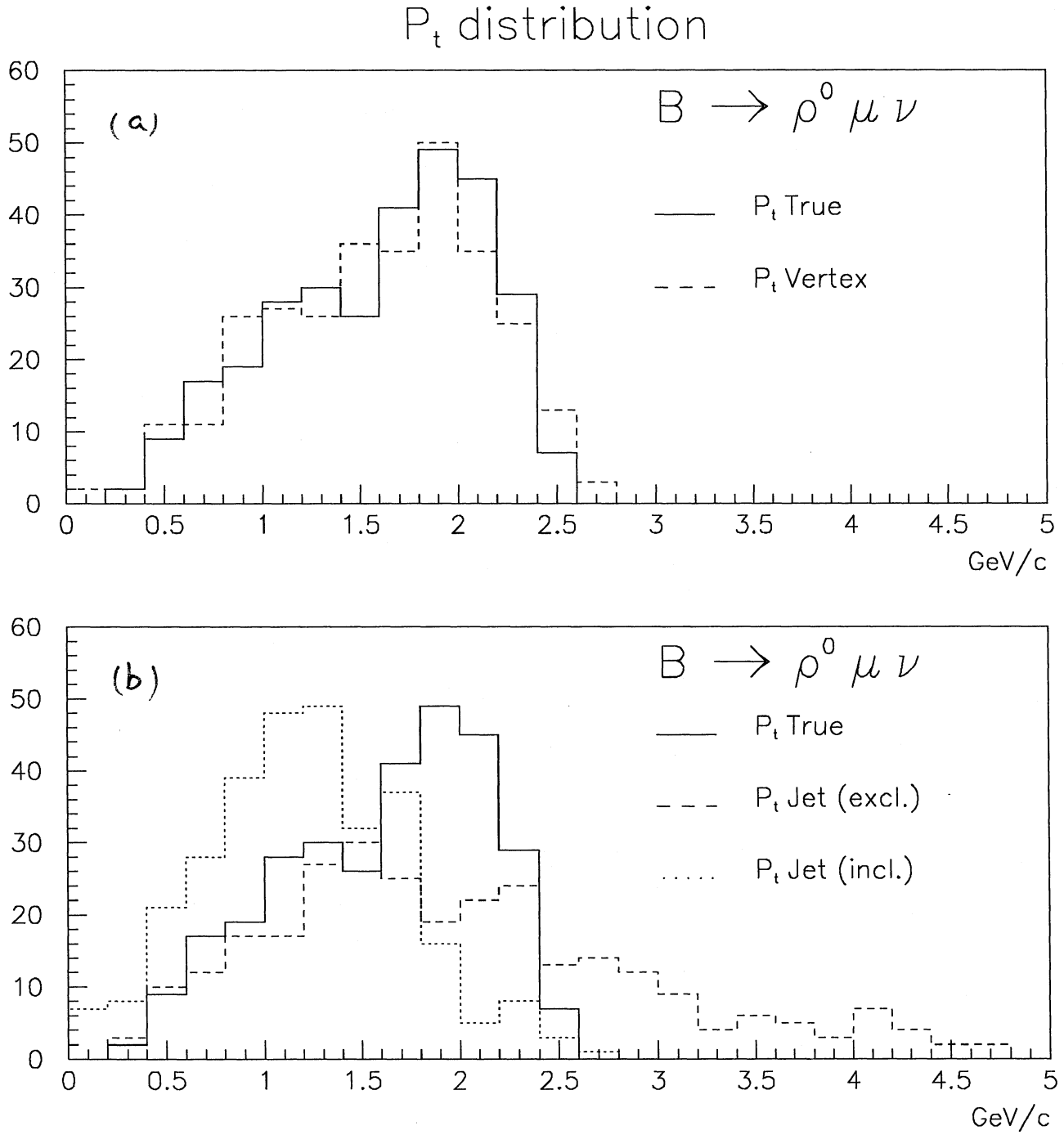

Figure 7: Distribution of reconstructed p_t, plotted with the true distribution, for $B \to \rho^0 l\nu$ events, (a) with the vertex p_t method and (b) the standard jet p_t methods.

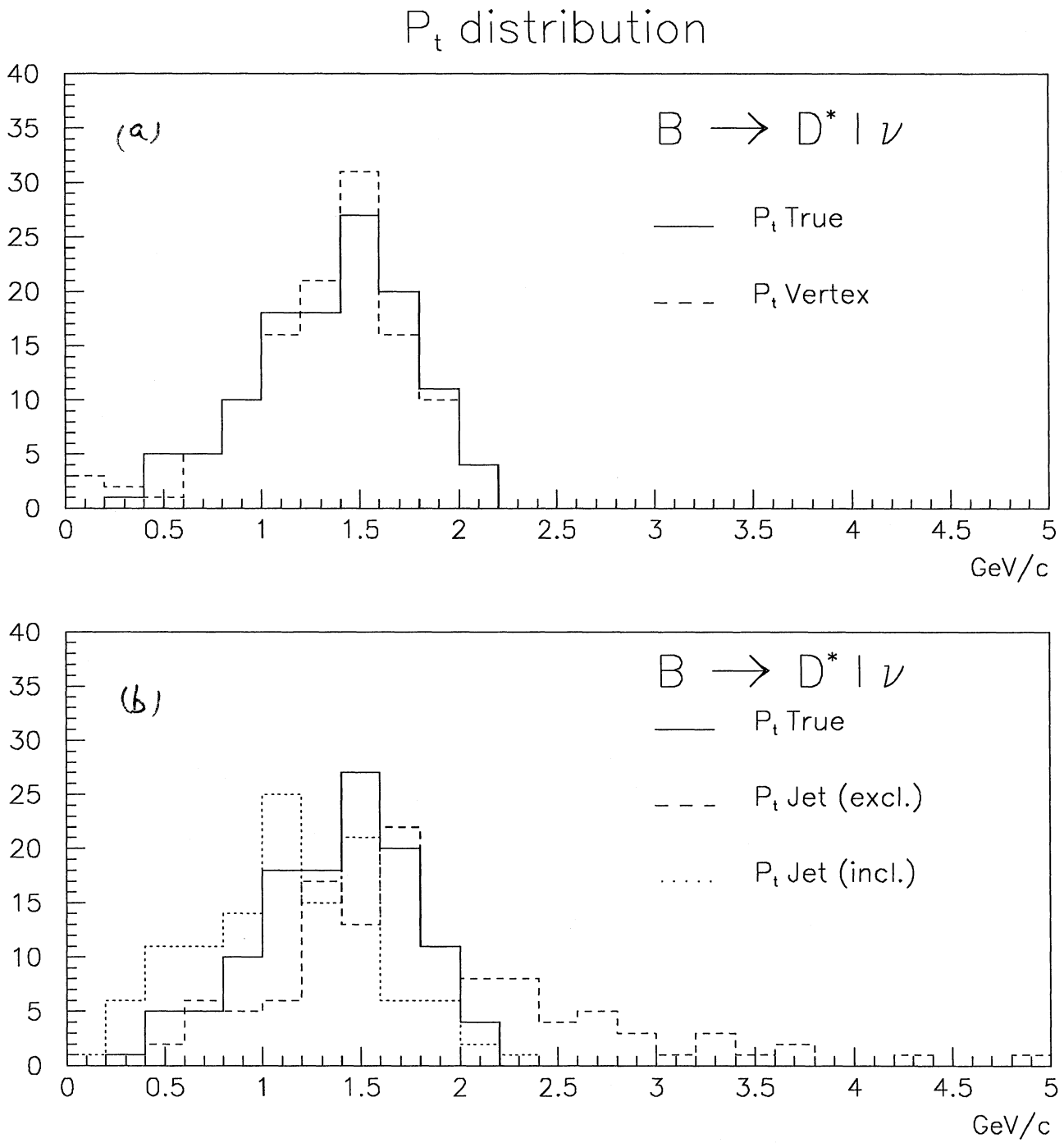

Figure 8: Distribution of reconstructed p_t, plotted with the true distribution, for $B \to D^{*+} l\nu$ events, (a) with the vertex p_t method and (b) the standard jet p_t methods.